Optics Letters

Diffraction by three-dimensional slit-shape curves: decomposition in terms of Airy and Pearcey functions

P. Martinez-Vara,[1] J. Silva Barranco,[2] S. I. De Los Santos G.,[2] J. Munoz-Lopez,[2] M. A. Torres-Rodriguez,[2] R. Suarez Xique,[1,3] and G. Martinez-Niconoff[2,*]

[1]Benemerita Universidad Autonoma de Puebla, Facultad de Ingenierias, Av. San Claudio s/n Puebla, Mexico
[2]Instituto Nacional de Astrofisica Optica y Electronica INAOE, Departamento de Optica, Puebla, Mexico
[3]Facultad de Ciencias Fisico Matematicas de la Benemerita Universidad Autonoma de Puebla, Apdo. Postal 1152, C. P. 72001 Puebla, Mexico
*Corresponding author: gmartin@inaoep.mx

Received 20 March 2015; revised 23 June 2015; accepted 24 June 2015; posted 1 July 2015 (Doc. ID 236534); published 22 July 2015

We analyze the diffraction field generated by coherent illumination of a three-dimensional transmittance characterized by a slit-shape curve. Generic features are obtained using the Frenet–Serret equations, which allow a decomposition of the optical field. The analysis is performed by describing the influence of the curvature and torsion on osculating, normal, and rectifying planes. We show that the diffracted field has a decomposition in three optical fields propagating along three optical axes that are mutually perpendicular. The decomposition is in terms of the *Pearcey* and *Airy* functions, and the generalized *Airy* function. Experimental results are shown.

OCIS codes: (050.1960) Diffraction theory; (050.5082) Phase space in wave optics.

http://dx.doi.org/10.1364/OL.40.003496

The diffraction field of planar transmittances containing a slit-shape curve generates caustic regions whose geometry can be calculated from the curvature function of the slit geometry [1], this optical field can be considered as a cylinder perpendicular to the transmittance function, the caustic region being the walls of the cylinder [2]. The caustic region separates two regions with different physical properties. One of them has a single-value phase function, while the other region has a multi-value phase function, which implies phase dislocations on the caustic region; consequently, different physical properties, such as entropy and vorticity, can be expected [3,4]. In addition, the walls of the cylinder present adiabatic features in the phase function, which physically means that caustic regions present no more wave behavior. Experimental evidence of this can be found in a previous work [5]. In this way, a very important topic to research is the establishment of the relation between the geometry of the different kinds of caustic regions with the transmittance function. The simplest case occurs when the optical field emerges from a planar transmittance containing a slit-shape curve, which has changes only in the curvature function [5–7]. In the present study, we go a step further and analyze the optical field when the boundary condition is a *three-dimensional (3-D)* slit-shape curve, i.e., the transmittance curve has curvature and torsion. These two geometrical properties imply that the diffraction field presents a more complicated structure.

The study is performed by describing the slit-shape curve using a trihedral reference system, characterized by the Frenet–Serret equations [8]. In this reference system, three mutually perpendicular planes are established: the osculating, the normal, and the rectifying planes. That the diffraction field can be separated as three optical fields, where each one has as a boundary condition a slit transmittance on each one of the trihedral planes, is inherited as a main consequence. To clarify previous assertions, we call attention to the following previous result. The diffraction fields associated with a transmittance containing a slit circular curve when it is illuminated with a plane wave at normal incidence generate nondiffracting fields whose geometry corresponds with a zero-order Bessel beam [9]. Modifying the illumination angle with a tilt in the transmittance, the diffraction field geometry changes dramatically, generating a cusped caustic region [5], as is shown in Fig. 1.

The cylindrical structure is easily identified; the cylinder basis is the cusp-shaped caustic region, and the multi-value region is formed by the inner points bounded by the caustic. This implies that, across the caustic region, the amplitude of the optical field is discontinuous, which generates an entropy process; more details concerning this behavior can be found in [10]. From the mathematical point of view, a differential transformation in the boundary condition generates optical fields that do not preserve the differentiability, meaning that the diffraction field depends strongly on the illumination configuration. To describe the diffraction field, an accurate reference system that takes the information of the geometric properties of the

0146-9592/15/153496-04$15/0$15.00

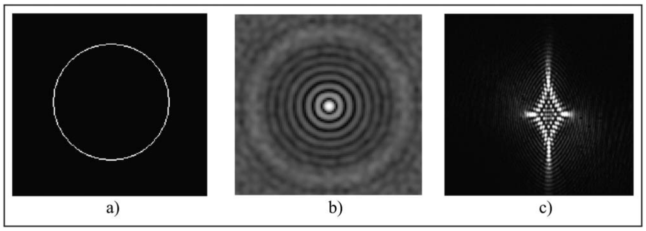

Fig. 1. (a) Transmittance characterized by a circular slit. (b) Diffraction field when the illumination is perpendicular to the transmittance, generating a zero-order Bessel beam. (c) Diffraction field when the incident angle is approximately 30°, generating a cusp-shaped caustic diffraction field.

transmittance is necessary. This can be established describing the *3-D* curve in parametric form:

$$\Psi(s) = (\xi(s), \eta(s), \zeta(s)), \tag{1}$$

where s is the arc length of the curve. The local reference system is identified using the Frenet–Serret equations:

$$\mathbf{T} = \frac{d\Psi(s)}{ds},\quad \frac{d\mathbf{T}}{ds} = \rho\mathbf{N},\quad \frac{d\mathbf{B}}{ds} = -\gamma\mathbf{N},\quad \frac{d\mathbf{N}}{ds} = -\rho\mathbf{T} + \gamma\mathbf{B}, \tag{2}$$

where ρ and γ are the curvature and torsion of the curve, respectively; $\mathbf{T}$ is the tangent vector; $\mathbf{N}$ is the normal vector; and $\mathbf{B} = \mathbf{T} \times \mathbf{N}$ is the bi-normal vector. These sets of vectors are mutually perpendicular having unitary modulus; this induces a local reference system known as the trihedral system [8]. From the set of vectors, three mutually orthogonal planes are identified. The vectors $\mathbf{T}$ and $\mathbf{N}$ generate the *osculating plane*, the $\mathbf{T}$ and $\mathbf{B}$ vectors generate the *rectifying plane*, and the vectors $\mathbf{N}$ and $\mathbf{B}$ generate the *normal plane*. Indeed, the tangent vector $\mathbf{T}$ defines the x-axis, the normal vector $\mathbf{N}$ defines the y-axis, and the bi-normal vector $\mathbf{B}$ defines the z-axis, as is sketched in Fig. 2. On the trihedral reference system, the Frenet–Serret equations given by Eq. (2) acquire the form

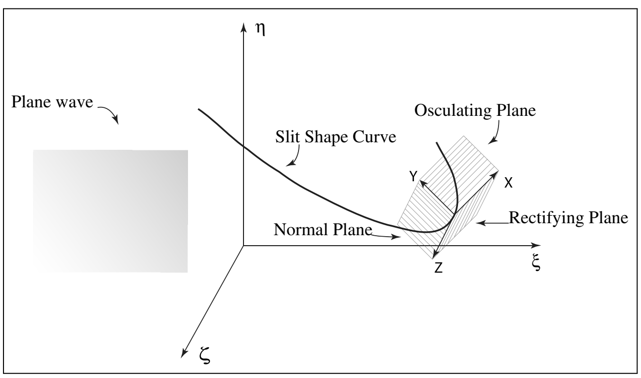

Fig. 2. Description of the *3-D* slit curve using the trihedral reference system.

$$\frac{dx}{ds} = 1,\qquad \frac{d^2x}{ds^2} = 0,\qquad \frac{d^3x}{ds^3} = -\rho^2, \tag{3}$$

$$\frac{dy}{ds} = 0,\qquad \frac{d^2y}{dy^2} = \rho,\qquad \frac{d^3y}{ds^3} = \rho', \tag{4}$$

$$\frac{dz}{ds} = 0,\qquad \frac{d^2z}{ds^2} = 0,\qquad \frac{d^3z}{ds^3} = \rho\gamma, \tag{5}$$

where ρ' is the derivative of the curvature with respect to the arc length. The curve solution on each plane is given as follows:

$$2y = \rho x^2, \tag{6}$$

$$6z = \rho\gamma x^3, \tag{7}$$

$$9\rho z^2 = 2\gamma^2 y^3. \tag{8}$$

The details of the results given by Eqs. (3)–(8) can be found in [8].

Previous comments indicate that the *3-D* transmittance can be detached in three transmittances that are mutually perpendicular. Equation (6) corresponds to the transmittance on the osculating plane; it is slit-shaped like a parabolic curve scaled by the curvature. The corresponding transmittance on a rectifying plane, Eq. (7), is slit-shaped like a cubic curve scaled by the product of curvature and torsion. The transmittance on the normal plane, Eq. (8), is slit-shaped like a cusp curve. For this decomposition in the three-dimensional boundary condition, the diffraction field can be described by the superposition of three optical fields, as is described below. The study is performed by illuminating the *3-D* slit curve with a plane wave. The wave vector $\mathbf{k}$ in the trihedral reference system has the components $\mathbf{k} = |k|(\cos\alpha, \cos\beta, \cos\chi)$, where (α, β, χ) are the angles between $\mathbf{k}$ and the corresponding axis (x, y, z). The diffraction field emerging from the osculating and rectifying planes is

$$\phi_{xy} = \iint \delta\left(y - \frac{\rho}{2}x^2\right) \frac{\exp(ikr\,\cos\alpha)}{r} \mathrm{d}x\mathrm{d}y, \tag{9}$$

$$\phi_{xz} = \iint \delta\left(z - \frac{\rho\gamma}{6}x^3\right) \frac{\exp(ikr\,\cos\beta)}{r} \mathrm{d}z\mathrm{d}x, \tag{10}$$

where r is the distance of propagation of the optical field, and δ is the Dirac delta function. We use this function because it make sense when its argument is zero, recovering Eqs. (6) and (7). Equation (9) corresponds to the Pearcey function, and it generates a cusped caustic. Equation (10) corresponds to the Airy function, and it generates a fold caustic [11]. In Fig. 3, we show the experimental results for these two cases. The diffracted field corresponding to a slit described by Eq. (8) is

$$\begin{aligned}\phi_{yz} &= \iint \delta\left(z^2 - \frac{2\gamma^2}{9\rho}y^3\right) \frac{\exp(ikr\,\cos\chi)}{r} \mathrm{d}z\mathrm{d}y \\ &= \int \exp\frac{i\pi}{\lambda x}(y^2 + ay^3) \exp\left(-i2\pi\frac{yy_0}{\lambda x}\right) \\ &\quad\times \cos\left(2\pi\frac{a^{1/2}y^{3/2}z_0}{\lambda x}\right) \mathrm{d}y,\end{aligned} \tag{11}$$

where $a = \frac{2\gamma^2}{9\rho}$. Grouping terms and expanding the cosine term in the power series, the amplitude function acquires the form of a series of generalized Airy functions $A_i(y, n)$:

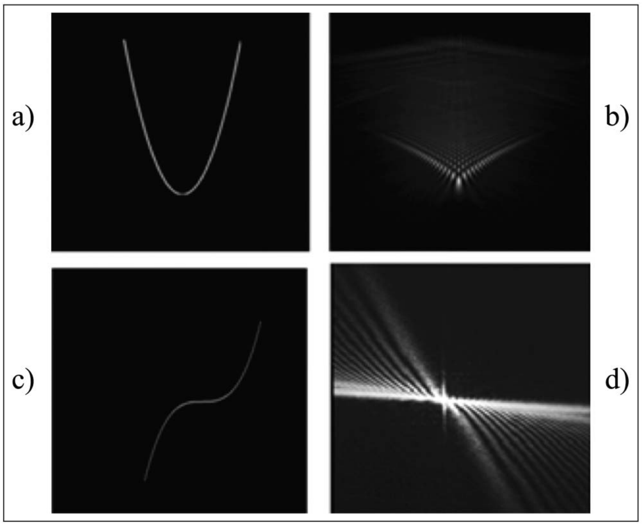

Fig. 3. Experimental results. (a), (b) Slit parabolic-shaped transmittance and its corresponding diffraction field. (c), (d) Slit cubic-shaped transmittance and its corresponding diffraction field. The transmittances are contained in a square of 0.5 cm per side.

$$\phi_{yz} = \sum_{n=0}^{\infty} C_n(z) A_i(y, n). \tag{12}$$

The convergence of the sum is not an easy mathematical problem; for this reason, we analyze the integral, keeping in mind a geometric point of view and using a geometrical theory of diffraction [12]. It must be noted that transmittance geometry can be considered as the joint of two curves, sharing a common point and generating the cusped shape. We interpret the optical field as the interference between two optical fields emerging from each branch. The description of the geometry of the interference fringes is obtained, taking as a reference the line **OS**, which is tangent to each branch in the cusped point, as is sketched in Fig. 4. As a consequence of the geometric theory of diffraction, the **k**-vector must be normal at each point on the slit curve [11,13]. This means that, in an arbitrary point on region 1 sketched in Fig. 5, only two linear trajectories are intersected; consequently, the diffraction field can be approximated locally as

$$\begin{aligned}\phi_{yz} &= \iint \delta(z^2 - ay^3)\frac{\exp(ikr\cos\chi)}{r}\,\mathrm{d}z\mathrm{d}y,\\ &\approx A\exp(i\mathbf{k}_1\cdot\mathbf{r}) + A\exp(i\mathbf{k}_2\cdot\mathbf{r}).\end{aligned} \tag{13}$$

The irradiance takes the form

$$I(x, y, z) = 2|A|^2(1 + \cos((\mathbf{k}_1 - \mathbf{k}_2)\cdot\mathbf{r})). \tag{14}$$

The global structure of the interference fringes depends on the $\Delta\mathbf{k} = \mathbf{k}_1 - \mathbf{k}_2$ vector, which takes the information of the curvature of the transmittance function. The geometry of the interference fringes can be deduced from the argument of the cosine term. Without loss of generality, we can consider only the regions of maximum interference given by

$$(\mathbf{k}_1 - \mathbf{k}_2)\cdot\mathbf{r} = 2m\pi, \tag{15}$$

where m is an integer that represents the interference order. The fringe geometry is obtained by plotting the $\Delta\mathbf{k}$ vector on the

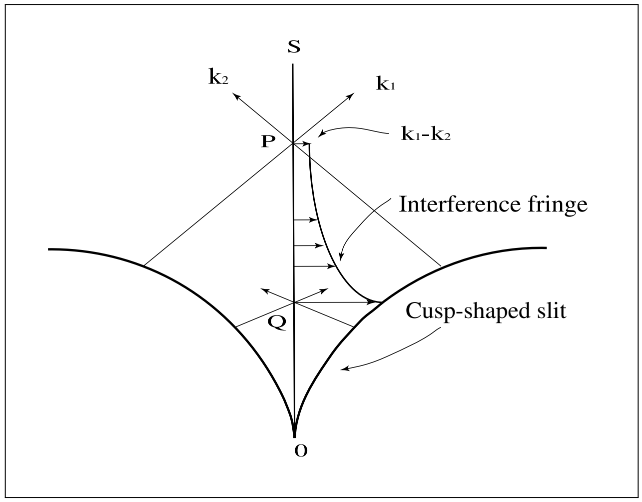

Fig. 4. Sketch to describe the diffracted field generated by the transmittance cusp-shaped slit. P and Q are two arbitrary points showing the $k_1 - k_2$ vector to describe the geometry of the interference fringe.

plane and joining all the points by a continuous curve as shown in Fig. 4. Counterpropagating the linear trajectories toward region 2, we predict the focusing region, which is generated by the envelope of all normal trajectories to each branch, as is sketched in Fig. 5. The superposition of the fringe geometry sketched in Fig. 4 with the geometry of the focusing region sketched in Fig. 5 justifies the experimental deltoid shape of the optical field shown in Fig. 6. In the common point of the transmittance, bifurcation effects are generated, which can be expected because, at this common point, the wave vector **k** has two possible directions; this occurs only in the neighborhood of the cusped point of the transmittance.

To explain the bifurcation effects, we use the fact that the irradiance function Eq. (14) satisfies the nonlinear partial differential equation:

$$\frac{\partial^2 I}{\partial a^2}\frac{\partial^2 I}{\partial b^2} - \left(\frac{\partial^2 I}{\partial a\partial b}\right)^2 = 0, \tag{16}$$

where $a = \Delta k_x$ and $b = \Delta k_y$. Equation (16) is the condition to generate an envelope curve for all points of the same phase, generating an interference fringe. Some generic features can be deduced, noting that the quadratic term is always positive;

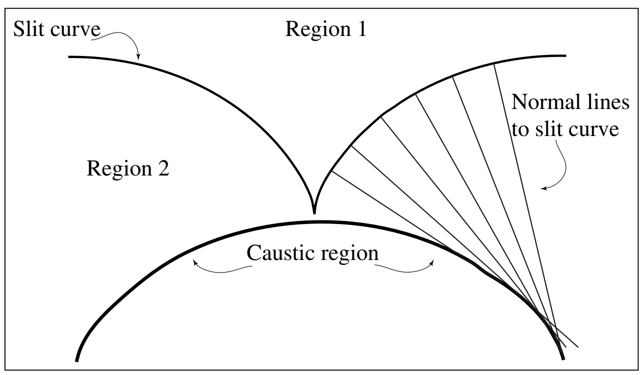

Fig. 5. Generation of the focusing region for a cusp-shaped slit.

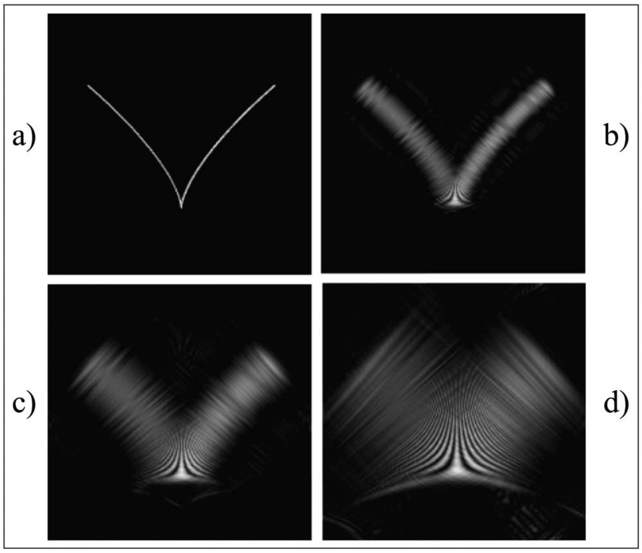

Fig. 6. (a) Cusp-shaped slit transmittance. (b)–(d) show the corresponding diffraction field detected on increasing propagation planes. The bifurcation effects are evident around the contact point. The transmittance is contained in a square of 0.5 cm per side.

consequently, the terms $\frac{\partial^2 I}{\partial a^2}$ and $\frac{\partial^2 I}{\partial b^2}$ must have the same sign. That is, both are negative or both are positive. This behavior has profound implications. In particular, the curvature function of the interference fringes must be a monotonic function without inflection points. When this requirement is not fulfilled, the optical field generates bifurcation effects. A formal analysis can be obtained from the stability of the irradiance function. Solving the differential equation Eq. (16) by means of separation of variables $I(a, b) = \xi(a)\eta(b)$, we generate the system of ordinary differential equations:

$$\xi \frac{d^2\xi}{da^2} = c\left(\frac{d\xi}{da}\right)^2, \qquad c\eta \frac{d^2\eta}{db^2} = \left(\frac{d\eta}{db}\right)^2, \tag{17}$$

where c is a coupling constant. The stability of the irradiance function is obtained by linearization of the system of Eq. (17). For this purpose, we use the following relations:

$$\frac{d\xi}{da} = \sigma\xi, \qquad \frac{d\eta}{db} = \tau\eta, \tag{18}$$

where σ and τ are constants. The system of differential equations, given by Eq. (17), acquires the form

$$\frac{d^2\xi}{da^2} = c_1\xi, \qquad \frac{d^2\eta}{db^2} = c_2\eta, \tag{19}$$

where the c_i constants must be positive in order for the interference to have real and positive values. The eigenvalues of the system Eq. (19) have two real values with opposite signs. As a consequence, the origin given by $a = 0$ and $b = 0$ is a repulsor point [14], which explains the bifurcation effects around the cusped point.

In this Letter, we presented the decomposition of the diffraction field generated by the illumination of a *3-D* slit transmittance. The study was performed using the Frenet–Serret equations, which allowed us to obtain three transmittances that were mutually perpendicular. Each transmittance takes the information of the curvature and torsion of the *3-D* transmittance. The transmittance function on the osculating plane generates an optical field whose amplitude is given by the Pearcey function, which generates a cusped caustic. On the normal plane, a cubic transmittance is generated, and the diffraction field corresponds with an Airy function, generating a fold caustic. Finally, on the rectifying plane, a transmittance kind cusped caustic slit is generated, and the diffraction field is a superposition of generalized Airy functions, whose geometry resembles a hyperbolic shape. This optical field is bounded by a curved focusing region generating a global shape deltoid. We also note that the complete diffraction field can be interpreted as a superposition of three optical fields, each propagating along one of three mutually perpendicular optical axes in the trihedral reference system. This study paves the way to incorporate other properties, such as polarization. In addition, it can be transferred to other physical fields, for example, in the generation of *1-D* plasmon fields [15], which can be obtained when the slit curve is replaced by a curved metal strip, being the curvature and torsion mechanism that allows the coupling between the illumination field and the plasmon field. This analysis will be presented in a forthcoming paper.

Acknowledgment. S. I. S. G., M. T. R., and J. S. B. are thankful for the support of CONACyT.

REFERENCES

1. G. Martinez-Niconoff, J. Carranza, and A. C. Rodriguez, Opt. Commun. **114**, 194 (1995).
2. S. M. Baumann, D. M. Kalb, L. H. MacMillan, and E. J. Galvez, Opt. Express **17**, 12 (2009).
3. Y. S. Kivshar and E. A. Ostrovskaya, Opt. Photon. News **12**(4), 24 (2001).
4. A. M. Yao and M. J. Padgett, Adv. Opt. Photon. **3**, 161 (2011).
5. G. Martinez-Niconoff, J. Munoz-Lopez, J. Silva-Barranco, A. Carbajal-Dominguez, and P. Martinez-Vara, Opt. Lett. **37**, 11 (2012).
6. M. S. Soskin, V. N. Gorshkov, M. V. Vasnetsov, J. T. Malos, and N. R. Heckenberg, Phys. Rev. A **56**, 4064 (1997).
7. E. Brasselet, G. Gervinskas, G. Seniutinas, and S. Juodkazis, Phys. Rev. Lett. **111**, 193901 (2013).
8. D. J. Struik, *Lectures on Classical Differential Geometry* (Dover, 1988), p. 23.
9. J. Durnin, J. Opt. Soc. Am. A. **4**, 651 (1987).
10. P. Prasad, *Nonlinear Hyperbolic Waves in Multi-Dimensions* (Chapman and Hall, 2001).
11. V. I. Arnold, *Singularities of Caustics and Wave Fronts* (Kluwer Academic, 1990).
12. J. B. Keller, J. Opt. Soc. Am. **52**, 2 (1962).
13. L. Elgoltz, *Differential Equations and Variational Calculus* (Mir, 1977).
14. E. J. Beltrami, *Mathematics for Dynamic Modeling*, 2nd ed. (Academic, 1987), p. 171.
15. D. R. Mason, S. G. Menabde, S. Yu, and N. Park, Sci. Rep. **4**, 4536 (2014).